Frank L. Martin

GENERALIZATION OF CONSTANT ABSOLUTE VORTICITY TRAJECTORIES.

UNITED STATES
NAVAL POSTGRADUATE SCHOOL

GENERALIZATION OF CONSTANT ABSOLUTE VORTICITY TRAJECTORIES

— By —

FRANK L. MARTIN

Associate Professor of Aerology

Research Paper No. 7

GENERALIZATION OF CONSTANT ABSOLUTE VORTICITY TRAJECTORIES

By

Frank L. Martin

U. S. Naval Postgraduate School
Monterey, California

15 February 1955

ABSTRACT

Previous studies of constant absolute vorticity (C.A.V.) trajectories have imposed the following limitations:

1. zero lateral shear
2. the trajectory is initiated from an inflexion
3. the flow is steady-state.

Limitation 1 may be generalized to constant lateral shear. Limitation 2 may be removed for both the plane and spherical trajectories. Limitation 3 is removed by an objective-type technique. The effect of lateral shear which varies along the trajectory is then considered, together with a quasi-geostrophic method of measuring it.

---

1. Introduction

In 1945, Starr [10] showed that the vertical component of isentropic absolute vorticity $f+\zeta_\theta$ satisfies the relationship

$$\frac{d}{dt}(f+\zeta_\theta) = -(f+\zeta_\theta)\,\nabla_{2\theta}\cdot\underline{V} \qquad (1)$$

where ζ_θ is the vertical component of relative isentropic vorticity, f the coriolis parameter and $\nabla_{2\theta}\cdot\underline{V}$ the isentropic divergence, that is the divergence of the horizontal wind in an isentropic surface. Starr derived (1) from the equations of motion using the quasi-Lagrangian coordinate θ in place of height. Haltiner [4] started from the equations of motion in Cartesian coordinates and derived (1) by transforming partial derivatives on a level surface into the corresponding derivatives on an isentropic chart. In (1) the individual operator d/dt must be measured along the initial isentropic surface and if this is done equation (1) may be considered to be quite exact.

In a specific situation, the isobaric surfaces might very nearly be substantial surfaces for a limited period of time. In this case equation (1) would apply with all subscripts θ replaced by p and the operator d/dt applied to trajectories drawn on contour height charts. Thus the form of the vorticity theorem in this case would be

$$\frac{d}{dt}(f+\zeta_p) = -(f+\zeta_p)\,\nabla_{2p}\cdot\underline{V} \qquad (2)$$

However the use of (2) would normally not be exact since there is involved the assumption that pressure is conservative.

Sutcliffe [11] has adapted the vorticity theorem to contour analysis and, dropping certain terms by virtue of their normal magnitudes, recommends the use of

$$\frac{d}{dt}(f+\zeta_p) = -f\,\nabla_{2p}\cdot\underline{V} \qquad (3)$$

Thus (1) is normally more exact than (2) or (3) in view of the assumptions and approximations involved in the latter two equations.

In the following discussion, our remarks will normally apply to trajectories based on equation (1) but in many cases, analogous statements will apply to trajectories based on equations (2) and (3).

2. Definition of the isentropic C.A.V. trajectory.

If the particle moves subject to the condition that the isentropic divergence be zero everywhere along the trajectory, then (1) can be integrated to give

$$f + \zeta_\theta = f_1 + \zeta_{\theta_1} = \text{constant} \qquad (4)$$

where the subscript 1 refers to an initial point (not necessarily an inflexion) along the trajectory. Under this condition, (4) essentially states that the vertical component of isentropic absolute vorticity is conserved along the trajectory.

According to Charney et al [2], the condition of zero isentropic divergence is most nearly realized along isentropic surfaces located near the 500 mb level. However, whether this condition is actually met with or not, the trajectory defined by (4) gives a convenient trajectory to which the actual trajectory may be compared, thereby affording an estimate of the distribution of divergence or convergence along the actual trajectory.

If in a given situation (2) or (3) affords a suitable approximation to the vorticity theorem for isobaric trajectories, then an isobaric C.A.V. trajectory is one for which the isobaric divergence $\nabla_p \cdot \underline{V} = 0$ and consequently

$$f + \zeta_p = f_1 + \zeta_{p_1} = \text{constant.}$$

In Rossby's original definition [8] of C.A.V. trajectories, in addition to the condition of zero divergence, the condition of barotropicity was also necessary. However there is no solenoid term in the vorticity

equation (1) as applied to isentropic surfaces and hence the only assumption made here is that of isentropic non-divergence.

3. General form of the equation governing C.A.V. trajectories

The vertical component of relative isentropic vorticity may be written in normal coordinates in the form

$$\zeta_\theta = \frac{V}{R_s} - \frac{\partial V}{\partial N}$$

where R_s is the horizontal radius of curvature of a streamline measured on the isentropic chart, V is the horizontal windspeed and N is the coordinate normal to the streamline. Then, using the Blaton relationship, equation (4) becomes

$$\frac{V}{R} - \frac{\partial \psi}{\partial t} - \frac{\partial V}{\partial N} + f = \frac{V}{R_{s_1}} - \frac{\partial V}{\partial N_1} + f_1 \qquad (5)$$

where $\partial\psi/\partial t$ is the local turning of the wind, positive for winds which back with time, and R is the horizontal radius of curvature of a trajectory drawn on an isentropic chart. The form of (5) tacitly assumes that the windspeed V remains constant along the trajectory.

4. Rossby-type C.A.V. trajectories

Originally Rossby selected parcels in the core of the jet as it appears on the given level. Thus in (5), he assumed that $\partial V/\partial N = \partial V/\partial N_1 = 0$. This condition can be generalized somewhat by assuming simply that

$$\frac{\partial V}{\partial N} = \left(\frac{\partial V}{\partial N}\right)_1 = \text{a constant not necessarily zero} \qquad (6)$$

along the isentropic C.A.V. trajectory. This assumption should be checked statistically, but for the present, suffice it to say that the assumption is as reasonable as to assume that a trajectory originating in a jet axis will remain within the jet. If the assumption (6) is made, then (5) may

be simplified to

$$\frac{V}{R} - \frac{\partial \psi}{\partial t} + f = \left(\frac{V}{R_s}\right)_1 + f_1 . \qquad (7)$$

A further characteristic of Rossby-type C.A.V. trajectories will be that of steady state, $\partial\psi/\partial t = 0$. In this case, streamlines and trajectories coincide and thus, with no local turning nor wind shear term in (7), the equation governing the C.A.V. trajectory is

$$\frac{V}{R} + f = \frac{V}{R_{s_1}} + f_1 \qquad (8)$$

which is essentially the equation treated originally by Rossby [8] and later by Bellamy (unpublished report). Bellamy solved (8) from an initial inflexion and constructed a slide rule to simplify the computations. Bellamy's slide rule was adaptable also to C.A.V. trajectories initiated from the trough and ridge in the streamline pattern but not from the points in between. Section 5 permits the construction of these trajectories from any initial point of known streamline curvature $1/R_{s_1}$, latitude φ_1, wind speed V and wind direction ψ_1. Furthermore this section develops clear-cut criteria, for the occurrence of loop-shaped C.A.V. trajectories together with the equation for such trajectories. Finally in Section 5b, the extension is made to spherical C.A.V. trajectories initiated from any arbitrary point. This then advances the earlier work of Platzman [6] and Wobus [12] who solved the spherical problem from an initial inflexion. Section 5 then fills certain gaps in connection with the present techniques of constructing C.A.V. trajectories. The results of Section 5 are then employed in Sections 6 and 7 where the steady-state and constant shear vorticity assumptions are removed.

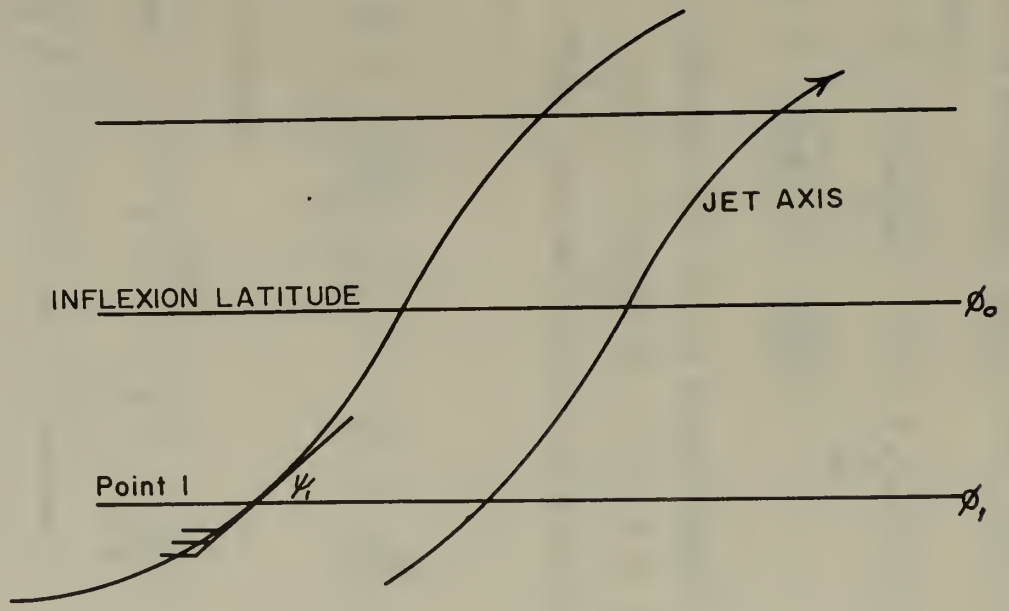

Fig. 1 Illustration of definition of Rossby C.A.V. trajectories. Initial point 1 need not be an inflexion and trajectory is not confined to jet axis.

5. Rossby-type C.A.V. trajectories from any arbitrary point.

The initial points of the C.A.V. trajectories to be discussed in this section are not confined to the jet axis, nor are they limited to inflexion points in the streamlines (fig. 1).

(a) C.A.V. trajectories in plane coordinates.

The equation for Rossby-type C.A.V. trajectories follows from (8) with R_{s1} relabeled R_1

$$\left.\begin{aligned} \frac{1}{R} &= \frac{1}{R_1} - \frac{(f-f_1)}{V}, \quad f-f_1 = 2\omega(\sin\varphi - \sin\varphi_1), \\ \frac{1}{R} &= \frac{d^2y}{dx^2}\left[1+\left(\frac{dy}{dx}\right)^2\right]^{-3/2}. \end{aligned}\right\} \quad (9)$$

Following Rossby, the term $f-f_1$ will be approximated by

$$f-f_1 = \frac{2\omega\cos\varphi_1}{a}(y-y_1) = \beta_1(y-y_1)$$

where $\beta_1 = 2\omega\cos\varphi_1/a$. Denoting dy/dx by q the curvature 1/R of (9) becomes

$$\frac{1}{R} = \frac{q\frac{dq}{dy}}{(1+q^2)^{3/2}} = \frac{1}{R_1} - \frac{\beta_1}{V}(y-y_1). \quad (10)$$

Integrating (10) leads to

$$\text{constant} - (1+q^2)^{-\frac{1}{2}} = \frac{y-y_1}{R_1} - \frac{\beta_1}{2V}(y-y_1)^2. \quad (11)$$

Furthermore $(1+q^2)^{-\frac{1}{2}} = \cos\psi$ so that (11) becomes

$$\cos\psi = \cos\psi_1 - \frac{(y-y_1)^2}{R_1} + \frac{(y-y_1)^2}{h^2}, \quad h^2 = \frac{2V}{\beta_1}, \quad (12)$$

whence

$$\cos\psi = F + \frac{1}{h^2}\left[y-y_1-\frac{h^2}{2R_1}\right]^2, \quad F = \cos\psi_1 - \frac{h^2}{4R_1^2}. \quad (13)$$

Equation (13) essentially determines the character of the C.A.V. trajectory. Thus for the special case $\psi_1 = 0$ (west wind), with h deter-

mined by the observed (or computed) wind speed and latitude, and for various values of cyclonic curvature, the possible C.A.V. trajectories are shown schematically in fig. 2.

In fig. 2, the necessary and sufficient condition for the existence of an inflexion between north and south bend points is that F represent a possible value of cosine. The various types of C.A.V. trajectories are listed below:

Trajectory AA: $4R_1^2(1+\cos\psi_1) < h^2$, no inflexion (14a)

Trajectory BB: $4R_1^2(1+\cos\psi_1) = h^2$, no inflexion (14b)

Trajectory CC: $4R_1^2(1+\cos\psi_1) > h^2 > 4R_1^2\cos\psi_1$, inflexion at I_C (14c)

Trajectory DD: $4R_1^2\cos\psi_1 > h^2$, inflexion at I_D (14d)

Note that an inflexion exists whenever $4R_1^2(1+\cos\psi) > h^2$. Case CC corresponds to an obtuse inflexion angle, $\cos\psi_0 < 0$ (and will be called a bent-back C.A.V. trajectory) while DD corresponds to a wavy-shaped trajectory, sinusoidal in form. Trajectory BB on reaching its poleward limit continues westward parallel to the latitude circle. Provided all other conditions are identical at the initial point, any trajectory more strongly curved than BB is a loop-shaped C.A.V. trajectory (eg. AA), whereas a trajectory less strongly curved (eg. CC or DD) will have an inflexion.

In those cases where an inflexion exists, its meridional distance from point 1, fig. 2, follows by setting the bracketed term of (13) equal to zero. Let this meridional distance be denoted Y. Then for the wavy-shaped and bent-back C.A.V. trajectories, the solution of the differential equation (13) can be made to depend upon the Rossby graphs [8] for C.A.V. trajectories originating from an inflexion. This is done simply

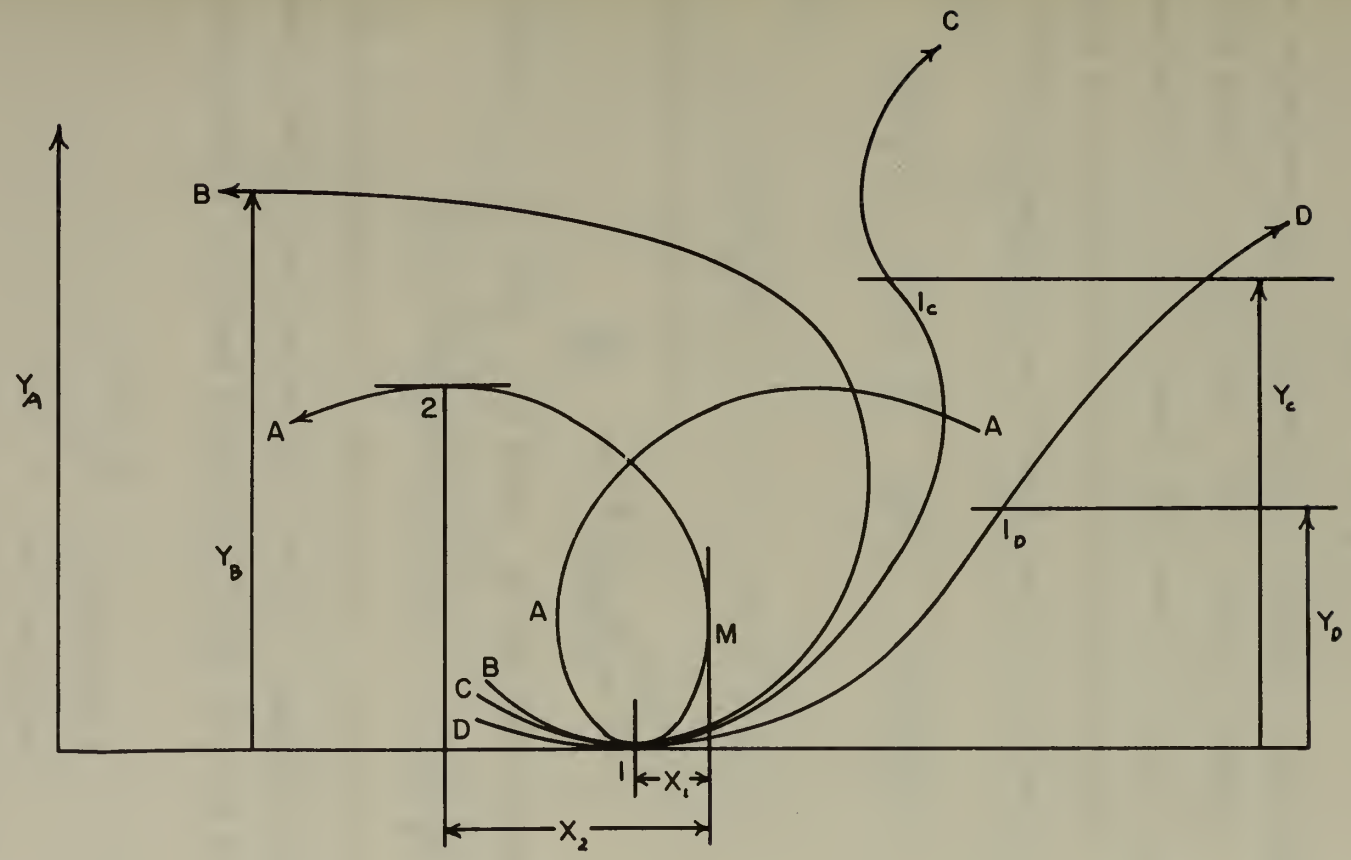

Fig. 2 Various types of Rossby C.A.V. trajectories which occur by varying trajectory curvature at initial point.

by using

$$\psi_0 = \cos^{-1}\left(\cos\psi_1 - \frac{h^2}{4R_1^2}\right),$$
$$Y = \frac{h^2}{2R_1} = \frac{h^2K_1}{2}, \qquad (15)$$

as the inflexional wind direction and inflexional displacement (meridionally from point 1), respectively. Thus with the windspeed, inflexional latitude and wind direction known, the characteristics of the C.A.V. trajectories are available with the aid of the Rossby graphs.

For the loop-shaped type of C.A.V. trajectory equation (13) may be written

$$(1+q^2)^{-\frac{1}{2}} = \cos\psi_1 - \frac{Y^2}{h^2} + \left(\frac{y-y_1-Y}{h}\right)^2. \qquad (16)$$

Setting

$$z^2 = \left(\frac{y-y_1-Y}{h}\right)^2 + 1 + \cos\psi_1 - \frac{Y^2}{h^2},$$

and solving (16) for $q = dy/dx$,

$$\frac{dy}{dx} = \frac{z(2-z^2)^{1/2}}{z^2-1}. \qquad (17)$$

Further $(y-y_1-Y)dy = h^2 z\,dz$ so that (17) becomes

$$dx = h(z^2-1)(2-z^2)^{-\frac{1}{2}}\left[z^2-\left(1+\cos\psi_1-\frac{Y^2}{h^2}\right)\right]^{-\frac{1}{2}} dz. \qquad (18)$$

For the loop-shaped C.A.V. trajectory it is desired to obtain the distances x_1 and x_2 from the point of vertical tangency ($dy/dx = \infty$), M, to both bend points of AA (where $dy/dx = 0$). Using (17) and (13) it follows that

$z^2 = 2$ at bend point 1

$z^2 = 0$ at bend point 2

$z^2 = 1$ at the point of vertical tangency, M.

Integration of (18) leads to

$$x_1 = h\int_{1/\sqrt{2}}^{1}(z^2-1)(2-z^2)^{-\frac{1}{2}}\left[z^2-\left(1+\cos\psi_1-\frac{Y^2}{h^2}\right)\right]^{-\frac{1}{2}} dz,$$
$$x_2 = h\int_{0}^{1}(z^2-1)(2-z^2)^{-\frac{1}{2}}\left[z^2-\left(1+\cos\psi_1-\frac{Y^2}{h^2}\right)\right]^{-\frac{1}{2}} dz. \qquad (19)$$

The integrals of (19) are essentially elliptic in nature. These will be evaluated under a variety of initial conditions governing h, ψ_1 , and $Y = K_1 h^2/2$ in some later publication. For the present it will suffice to develop some semi-qualitative aspects of loop-shaped C.A.V. trajectories. Setting $\cos\psi = -1$ in (13) one obtains the condition which the meridional distance from point 1 to bend-point 2 must satisfy

$$\left(\frac{y - y_1 - Y}{h}\right)^2 + 1 + \cos\psi_1 - \frac{Y^2}{h^2} = 0. \qquad (20)$$

The solution of (20) is

$$y - y_1 = Y \pm Y\left[1 - \frac{4R_1^2(1+\cos\psi_1)}{h^2}\right]^{1/2}. \qquad (21)$$

In (21) only the minus sign is permissible since the loop-type C.A.V. trajectory cannot go as far poleward as $y - y_1 = Y$ with condition (14a) holding. Fig. 2 illustrates the application of (21) for the special case $\psi_1 = 0^\circ$ (west winds at initial point 1). It will be noted that $Y_A > Y_B > Y_C > Y_D$ for the case illustrated where only the curvature at point 1 has been allowed to vary.

(b) C.A.V. trajectories in spherical coordinates

Equation (8) will be expressed in the form

$$VK_g = -f + f_1 + VK_{g1}, \quad K_g = \frac{1}{R}, \qquad (22)$$

in order to emphasize that the curvatures K_g, K_{g1} are actually geodesic curvatures. Platzman [6] has shown that, if a is the radius of the earth,

$$K_g = -\frac{1}{a}\,\frac{d(\cos\psi\cos\varphi)}{d(\sin\varphi)}, \qquad (23)$$

where ψ is the wind direction measured relative to a latitude circle on a Lambert conformal or polar stereographic map. In both of these map projections, very little error is introduced by writing the geodesic curvature

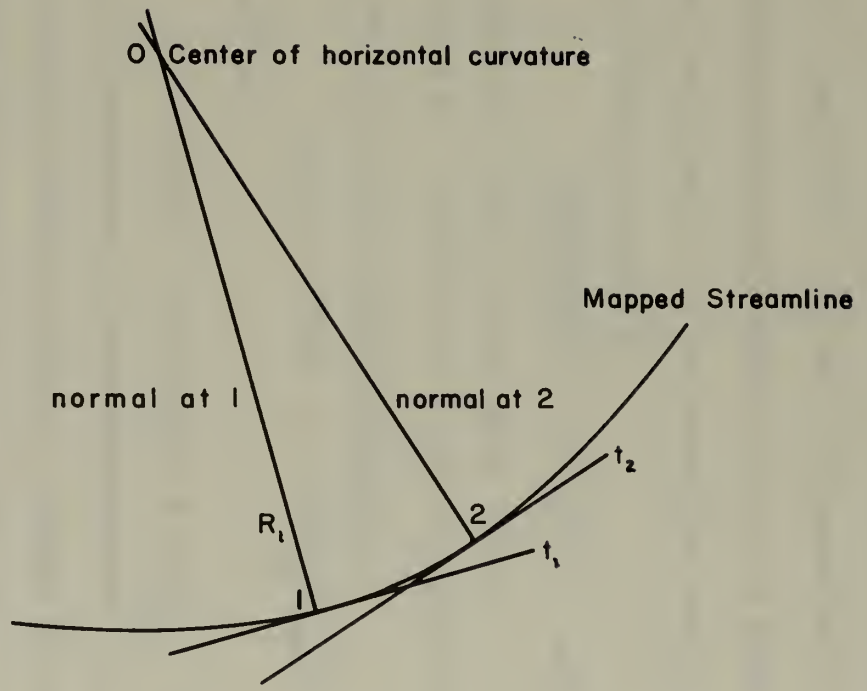

Fig. 3 Measuring the mapped streamline curvature.

Kg as the product of a map-scale factor and the plane curvature of the mapped trajectory. The geodesic curvature $K_{g1} = 1/R_1$ is then essentially equal to the curvature at the initial point of the mapped streamline provided one uses the units of (deg lat)$^{-1}$. The radius of curvature R_1 of the streamline is by definition very nearly equal to that of a circle passing through point 1 and some nearby point 2 on the streamline (see fig. 3).

Combining (22) and (23) leads to

$$\frac{d(\cos\psi\cos\varphi)}{d(\sin\varphi)} = \frac{(f-f_1)a}{V} - aK_{g1}, \qquad (24)$$

which, upon integration from $\varphi=\varphi_1$ to $\varphi=\varphi$ gives

$$\cos\psi\cos\varphi = \cos\psi_1\cos\varphi_1 + \frac{\omega a}{V}(\sin\varphi-\sin\varphi_1)^2 - aK_{g1}(\sin\varphi-\sin\varphi_1). \qquad (25)$$

Again, making use of the first order approximation

$$\sin\varphi - \sin\varphi_1 = \frac{\cos\varphi_1\,(y-y_1)}{a} \qquad (26)$$

one obtains from (25),

$$\cos\psi = \sec\varphi\cos\varphi_1\left[\cos\psi_1 + \left(\frac{y-y_1}{h}\right)^2 - \left(\frac{y-y_1}{R_1}\right)\right]. \qquad (27)$$

Actually it is unnecessary to make approximation (26) in order to determine the north and south bend points. Platzman [6] solved equation (27) for the latitude φ of the bend points without approximation when point 1 referred to an inflexion point. In most cases, however, the use of the linear approximation (26) will not seriously affect the accuracy of the C.A.V. trajectory, especially since (26) and (27) will not be used beyond the inflexion latitude (if one exists). Our point of view will be similar to that of the plane case, namely, to use the linear approximation in order to determine the inflexion latitude and direction and then use available tables (involving no approximations) such as those of [6] and [12] in order to construct the remainder of the C.A.V. trajectory.

Let us next determine the condition that the C.A.V. trajectory be loop-shaped. Setting $\cos\psi = -1$ and $\cos\varphi = \cos\varphi_1 - \sin\varphi_1\,(y-y_1)/a$, one

obtains

$$\left(\frac{y-y_1}{h}\right)^2 - \frac{y-y_1}{R_1} + \cos\psi_1 + 1 - \frac{\tan\varphi_1}{a}(y-y_1) = 0,$$

and finally

$$\left(\frac{y-y_1}{h}\right)^2 - (y-y_1)\left[K_{g_1} + \frac{\tan\varphi_1}{a}\right] + 1 + \cos\psi_1 = 0. \tag{28}$$

Equation (28) would normally have two solutions provided

$$\left(K_{g_1} + \frac{\tan\varphi_1}{a}\right)^2 h^2 - 4(1+\cos\psi_1) > 0 \tag{29}$$

which is similar to the condition for the loop-shaped C.A.V. trajectory of fig. 2. Note that the modification for sphericity is obtained from (14a) by replacing K_1 by $(K_{g1}) + \tan\varphi_1/a$. If (29) holds, only one solution is possible, namely

$$y - y_1 = Y - Y\left[1 - \frac{4(1+\cos\psi_1)}{h^2(K_{g_1} + \frac{\tan\varphi_1}{a})^2}\right]^{1/2}, \quad Y = \frac{h^2}{2}\left(K_{g_1} + \frac{\tan\varphi_1}{a}\right), \tag{30}$$

analogous to (21). In (30), a possible solution corresponding to the plus sign before the radical has been discarded by virtue of reasoning similar to that following (21).

If the left side of (29) is negative, that is if

$$4(1+\cos\psi_1) > \left(K_{g_1} + \frac{\tan\varphi_1}{a}\right)^2 h^2, \tag{31}$$

then the C.A.V. trajectory has an inflexion point. In this case the meridional displacement of the inflexion from point 1 is determined by (22) with $K_g = 0$. This leads to

$$\frac{2\omega\cos\varphi_1(y_0 - y_1)}{aV} - K_{g_1} = 0$$

or

$$y_0 - y_1 = \frac{K_{g_1}V}{B_1} = \frac{K_{g_1}h^2}{2} \tag{32}$$

as the meridional displacement to the inflexion.

For C.A.V. trajectories having an inflexion the solution of (27) may be made to depend upon the tables [12] deduced from "wiggle-wagon" runs

initiated from an inflexion. The differential equation solved by the Wobus differential analyzer is essentially (27) with the initial point at the inflexion latitude φ_0, that is

$$\cos\psi = \sec\varphi \cos\varphi_0 \left[\cos\psi_0 + \left(\frac{y-y_0}{h_0}\right)^2\right], \quad h_0^2 = \frac{2V}{\beta_0}, \tag{33}$$

with ψ_0 the inflexional wind direction. Equation (27) which represents the C.A.V. trajectory from an arbitrary initial point may be written

$$\cos\psi = \sec\varphi \cos\varphi_1 \left[\cos\psi_1 - \frac{K_{g_1}^2 h^2}{4} + \frac{1}{h^2}\left(y - y_1 - \frac{K_{g_1} h^2}{2}\right)^2\right], \quad h^2 = \frac{2V}{\beta_1}. \tag{34}$$

Since, by (32), $y_1 + \frac{K_{g_1} h^2}{2} = y_0$ is the ordinate which gives the latitude of the inflexion, (34) may be written

$$\cos\psi = \sec\varphi \cos\varphi_0 \left[\frac{\cos\varphi_1}{\cos\varphi_0}\left(\cos\psi_1 - \frac{K_{g_1}^2 h^2}{4}\right) + \left(\frac{y-y_0}{h}\right)^2 \frac{\cos^2\varphi_1}{\cos^2\varphi_0}\right]. \tag{35}$$

The last equation[1] represents the C.A.V. trajectory (34) expressed in terms of its inflexional characteristics. These are

$$\begin{aligned} &\text{inflexional latitude:} && \varphi_0 = \varphi_1 + K_{g_1} h^2/2a \\ &\text{inflexional direction:} && \cos\psi_0 = \frac{\cos\varphi_1}{\cos\varphi_0}\left(\cos\psi_1 - \frac{K_{g_1}^2 h^2}{4}\right) \end{aligned} \tag{36}$$

Nomograms solving (36) will be presented in a later publication. From (36), together with the known V, one has the inflexional data with which to enter tables [12]. In order to construct this C.A.V. trajectory, first construct any C.A.V. trajectory satisfying the necessary inflexional data φ_0 and ψ_0, in fig. 4, and then displace it eastward or westward so that the displaced trajectory passes through the initial point 1 with the desired direction ψ_1.

6. Unsteady C.A.V. trajectories

The motion considered in this section is that of unsteady $(\partial\psi/\partial t \neq 0)$ horizontal flow in terms of rectangular coordinates. However the horizontal

---

[1] It may be shown, by returning to equations (25) and (32), and avoiding the linear approximation (26) to the very last step that the ratio $\cos^2\varphi_1/\cos^2\varphi_0$ on the right side of (35) may be replaced by 1.

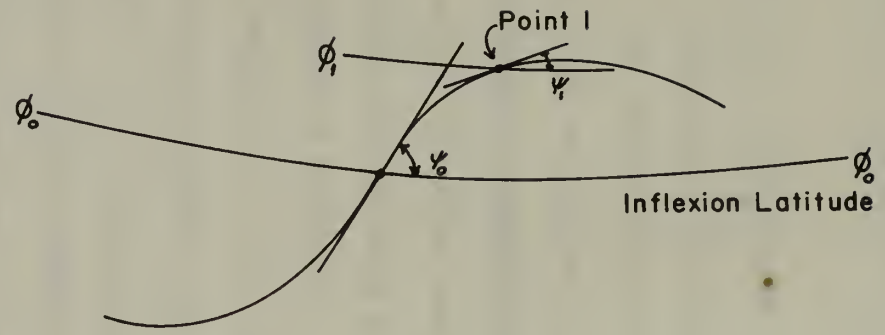

Fig. 4 Construction, using inflexional characteristics, of spherical-type C.A.V. trajectory from arbitrary initial point.

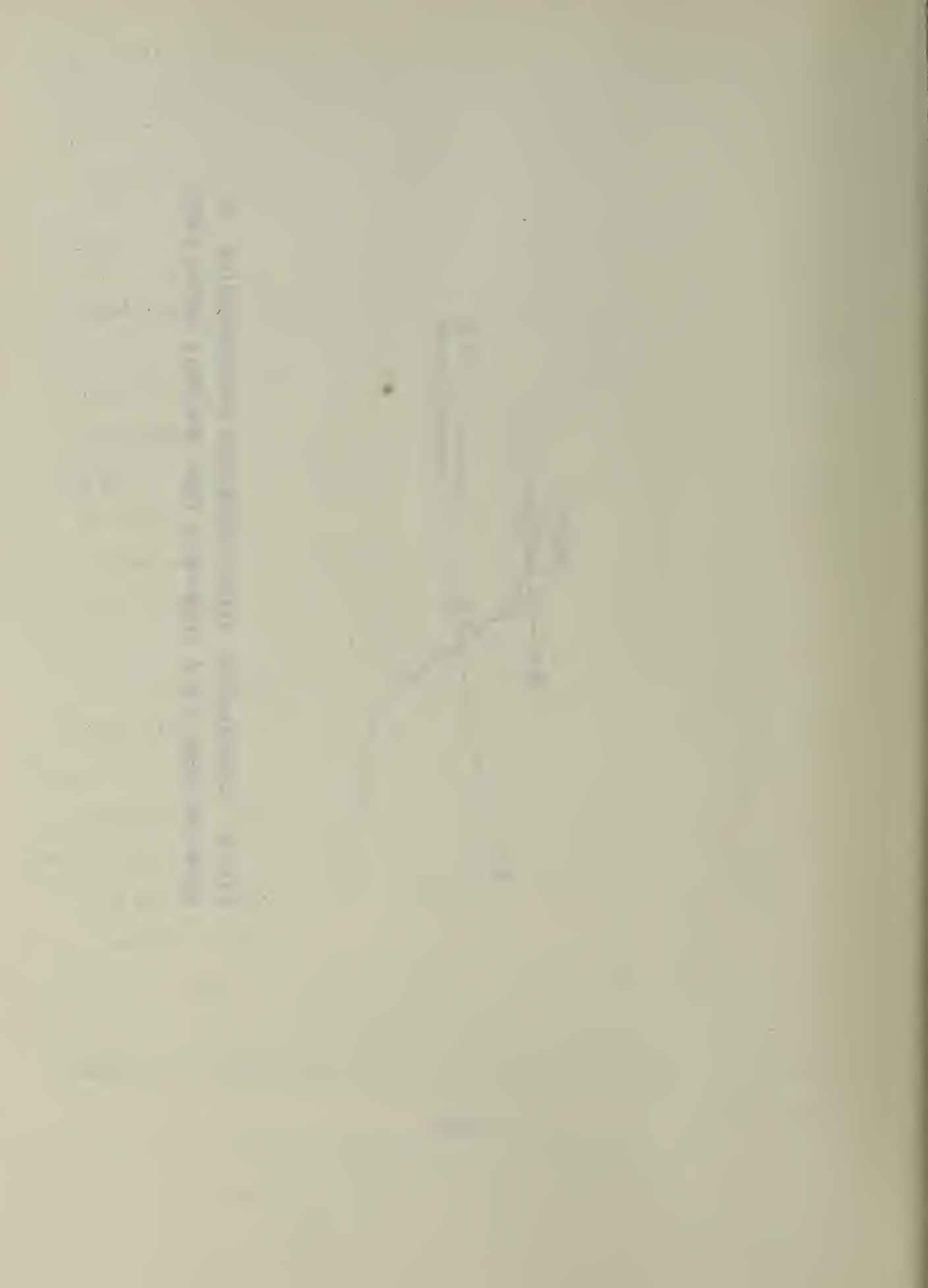

shear of the isentropic flow will be assumed constant along the trajectory so that (7) is the governing equation of this section. Assuming that the particle starts initially from an inflexion, $1/R_1 = 0$ and $f_1 = f_0$, the subscript zero denoting the inflexion latitude. Thus equation (7) takes the form

$$\frac{V}{R} - \frac{\partial \psi}{\partial t} = -(f - f_0) = -\beta_0 (y - y_0). \qquad (37)$$

It will also be assumed that the unsteady C.A.V. trajectory is not loop-shaped.

Consider the Rossby C.A.V. trajectory to be a first approximation to the true unsteady C.A.V. trajectory and one which will give a representative estimate of $\partial\psi/\partial t$. The situation is illustrated in fig. 5. In general the following prodecure may be applied in specific cases whether or not the streamlines have sinusoidal characteristics such as wave length and amplitude. However in order to deduce some general conclusions, such characteristics are assumed in the following discussion.

The usual case of progressive streamlines is depicted in fig. 5. Synoptically this usually requires $L < L_s$, where L is the wave length of the streamline[2] through inflexion latitude φ_0 and L_s is that of the Rossby C.A.V. trajectory initiated at the inflexion point O, with the direction of the streamline at O. As Grant [5] has indicated, such a trajectory will generally have a greater amplitude than that of the contiguous streamline, and this is the case depicted in fig. 5. However the method presented here applies regardless of the comparison between wave lengths.

---

[2]Throughout this section "streamline" is used as a synonym for an isoline of the isentropic stream function.

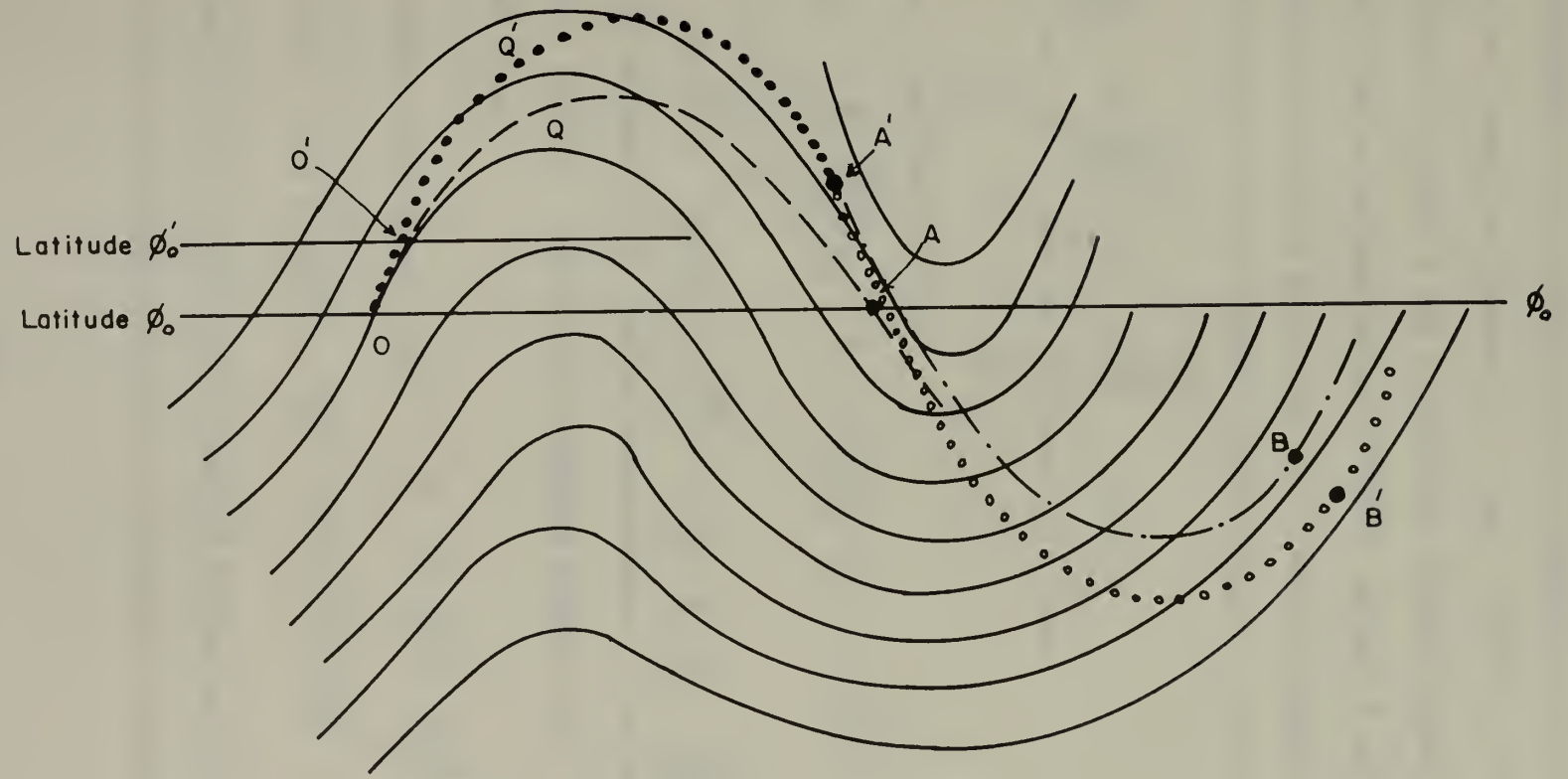

Fig. 5 Unsteady C.A.V. trajectories drawn by successive approximations.

In order to determine $\partial\psi/\partial t$ at any point Q from fig. 5, the cross-streamline angle $\Delta\psi$ is measured using the Rossby trajectory OQA (dashed curve) as a first approximation to the unsteady C.A.V. trajectory. The time Δt is that necessary to travel the distance OQ. Then $\partial\psi/\partial t \doteq \Delta\psi/\Delta t$. In fig. 5, $\partial\psi/\partial t = 0$ at point A and is positive (backing) from O to A. It will be assumed that an average value of $\partial\psi/\partial t$ between O and A gives a closer approximation to the true trajectory (37) than the Rossby C.A.V. trajectory. The average value of $\partial\psi/\partial t$ between O and A, fig. 5, is given by

$$\frac{\partial\psi}{\partial t} \doteq \overline{\left(\frac{\partial\psi}{\partial t}\right)} = \alpha V, \qquad \alpha > 0 \tag{38}$$

which also defines α. Setting (38) into (37) gives

$$\frac{V}{R} - \alpha V = -\beta_0 (y - y_0). \tag{39}$$

Equation (39) may be modified to form

$$\frac{1}{R} = \frac{q\, dq/dy}{(1+q^2)^{3/2}} = -\frac{\beta_0}{V}\left(y - y_0 - \alpha\beta_0^{-1} V\right), \tag{40}$$

a first integral of which is

$$\cos\psi = \cos\psi_0 - \frac{\alpha^2 h_0^2}{4} + \frac{1}{h_0^2}\left(y - y_0 - \alpha\frac{h_0}{2}\right)^2. \tag{41}$$

Equation (41) represents the desired approximation to the unsteady C.A.V. trajectory. From its form it is a <u>modified</u> Rossby C.A.V. trajectory having wind speed V and

$$\left.\begin{aligned} &\text{inflexional latitude,} && \varphi_0' = \varphi_0 + \frac{1}{a}\left(\frac{\alpha h_0^2}{2}\right), \\ &\text{inflexional wind direction,} && \psi_0' = \cos^{-1}\left(\cos\psi_0 - \frac{\alpha^2 h_0^2}{4}\right) \end{aligned}\right\} \tag{42}$$

This modified Rossby C.A.V. trajectory is depicted by the curve OO'Q'A' (dotted curve in fig. 5), and also in fig. 6 (in somewhat enlarged version).

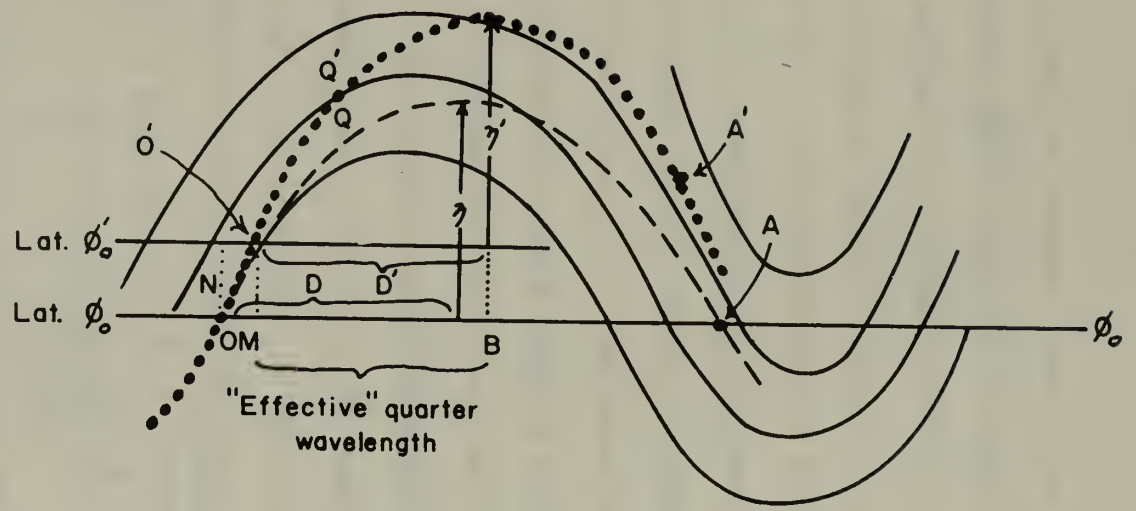

Fig. 6 Inflexional characteristics of the unsteady C.A.V. trajectory obtained as a modified Rossby C.A.V. trajectory.

The point A' has been selected along OO'Q'A' as the point where $\partial\psi/\partial t = 0$, that is where the nearest streamline parallels the trajectory satisfying (41) and (42).

Since $\partial\psi/\partial t$ is positive between O and A, the procedure of spreading uniform cyclonic turning $\partial\psi/\partial t$ along OO'Q'A' gives this curve less anti-cyclonic rotation latitude for latitude than OQA. This procedure has also induced cyclonic curvature at point O of OO'Q'A', since O' is its inflexion point. If η' and η are the amplitudes of O'Q'A', OQA, respectively and if D' and D are the corresponding quarter-wave lengths (see fig. 6), it will be shown below that $\eta' > \eta$, $D' < D$. However, since the quarter wave length D of the Rossby C.A.V. trajectory begins at O, the "effective" quarter wave length of OO'Q'A' should begin at O rather than O' and is D' + OM in fig. 6. Likewise the "effective" amplitude is $\eta' + \varphi_0' - \varphi_0$. The parameters η', D' of O'Q'A' are determinable from the Rossby graphs [9] using the inflexion point data (42). No general conclusion can be drawn as to whether D' + OM is greater or less than D.

The relationships between η', η and D', D will now be derived. From (41), it follows that η is given by $\eta = h_0\sqrt{1-\cos\psi_0}$ so that

$$\frac{\eta'}{\eta} = \left(\frac{1-\cos\psi_0'}{1-\cos\psi_0}\right)^{1/2} = \frac{\sin\frac{\psi_0'}{2}}{\sin\frac{\psi_0}{2}} > 1.$$

The quarter wave length D of the Rossby C.A.V. trajectory follows from (41) by a method similar to that of Rossby [8, p. 82] and is

$$\frac{D}{h} = \int_{\sqrt{1+\cos\psi_0}}^{\sqrt{2}} \frac{(z^2-1)\,dz}{(2-z^2)^{1/2}(z^2-1-\cos\psi_0)^{1/2}}, \quad z^2 = \left(\frac{y-y_0}{h_0}\right)^2 + 1 + \cos\psi_0. \tag{43}$$

In (43), ψ_0 is the inflexional wind direction at O, $z^2 = 2$ at the ridge and $z^2 = 1+\cos\psi_0$ at the inflexion point O of OQA. An analogous equation for D' of the unsteady C.A.V. trajectory O'Q'A' leads to (44) with ψ_0

replaced by ψ_0'. Thus

$$\frac{D'}{h} = \int_{\sqrt{1+\cos\psi_0'}}^{\sqrt{2}} \frac{(z^2-1)\,dz}{(2-z^2)^{\frac{1}{2}}(z^2-1-\cos\psi_0')}, \qquad z^2 = \left(\frac{y-y_0}{h_0}\right)^2 + 1 + \cos\psi_0' \tag{44}$$

Rossby [9, p. 273] has denoted the integral of the right side of (43) by the notation

$$\frac{\pi}{2\sqrt{2}} F_1(\psi_0)$$

with $F_1(\psi_0)$ shown in his Fig. 118 as a decreasing function of ψ_0. Since (44) is a special case of (43) with $\psi_0' > \psi_0$, it follows that $D' < D$.

Expressions for the inflexional corrections (42) will now be derived. Defining $\Delta\psi = \psi_0' - \psi_0$, consider

$$\cos(\psi_0 + \Delta\psi) = \cos\psi_0 - \frac{\alpha^2 h_0^2}{4}$$

from which it follows to a good degree of approximation, that

$$\sin\psi_0 \, \Delta\psi = \frac{\alpha^2 h_0^2}{4}. \tag{45}$$

Moreover

$$\frac{\alpha^2 h_0^2}{4} = \frac{(\partial\psi/\partial t)^2}{4V^2} \frac{2Va}{2\omega\cos\varphi_0} = \frac{(\partial\psi/\partial t)^2 a}{2V(2\omega\cos\varphi_0)}, \tag{46}$$

$$\varphi_0' - \varphi_0 = \frac{1}{2a}(\alpha h_0^2) = \frac{1}{2a} \frac{(\partial\psi/\partial t)}{V} \frac{2aV}{2\omega\cos\varphi_0} = \frac{\partial\psi/\partial t}{2\omega\cos\varphi_0}. \tag{47}$$

Selecting typical values of the parameters, as follows

$$(\partial\psi/\partial t) = 20^\circ (12 \text{ hours})^{-1} = 8.1 \times 10^{-6} \text{ sec}^{-1},$$

$$V = 50 \text{ mps} = 5000 \text{ cm sec}^{-1},$$

$$2\omega\cos\varphi_0 = 10^{-4} \text{ sec}^{-1} \quad (\text{latitude } \varphi_0 = 47^\circ),$$

$$a = 6.371 \times 10^8 \text{ cm}.$$

the value obtained on the right side of (46) is .042. From (45) the value of $\Delta\psi$ (with $\sin\psi_0 = .866$) is $\Delta\psi = .047$ or $\psi_0' = 62.9°$. From Rossby [9, p. 275], this gives a reduction in quarter wave length D' of approximately 3% compared to D for the corresponding Rossby C.A.V. trajectory for $\psi_0 = 60°$. Furthermore, the right side of (47) has the value $\varphi_0' - \varphi_0 = .081$ for the parameters used so that the poleward shift in inflexional latitude, fig. 6, is approximately 5° latitude.

The second approximation OO'Q'A' to the unsteady C.A.V. trajectory may be extended beyond the point A' by a continuation of the process used on the first leg OO'Q'A'. A Rossby C.A.V. trajectory A'B (the dot-dash curve in fig. 5) initiated at A' (where $\partial\psi/\partial t = 0$) has $K_1 = K_{S1}$, the curvature of the interpolated streamline which touches OO'Q'A' at A'. The other end point B is also characterized by tangency of the Rossby C.A.V. trajectory and an (interpolated) streamline so that $\partial\psi/\partial t = 0$ at B. Between A' and B, a representative mean value

$$\overline{\left(\frac{\partial\psi}{\partial t}\right)} = \alpha_1 V \tag{48}$$

may be computed, where α_1 is negative (winds veering with time) in fig. 5, a fact which is essentially equivalent to the statement that the original Rossby C.A.V. trajectory had greater amplitude than the contiguous streamline. Using (48), equation (7) takes the form

$$\frac{1}{R} = \frac{g\, dq/dy}{(f+q^2)^{3/2}} = K_1 + \alpha_1 - \frac{2}{h_1^2}(y - y_1). \tag{49}$$

The first integral of (49) is

$$\cos\psi = \cos\psi_1 - \frac{(K_1+\alpha_1)^2 h_1^2}{4} + \frac{1}{h_1^2}\left[y - y_1 - \frac{(K_1+\alpha_1)h_1^2}{2}\right]^2, \tag{50}$$

a relationship which is satisfied along the "second leg" A'B', the curve

delineated by small open circles in fig. 5. The form of (50) indicates that this second leg of the unsteady C.A.V. trajectory may be drawn as a modified Rossby C.A.V. trajectory having windspeed V and

$$\text{inflexion latitude: } \varphi_{1,0}' = \frac{1}{a}\left[y_1 + \frac{(K_1+\alpha_1)h_1^2}{2}\right],$$
$$\text{inflexion direction: } \cos\psi_{1,0}' = \cos\psi_1 - \frac{(K_1+\alpha_1)^2 h_1^2}{4}. \qquad (51)$$

The inflexional wind direction $\psi_{1,0}$ for the Rossby C.A.V. trajectory A'B follows from (51) on setting $\alpha_1 = 0$. However for trajectory A'B', K_1 and α_1 are both negative so that $\psi_{1,0}' > \psi_{1,0}$. Denoting the quarter wave lengths of A'B' and A'B, respectively, by D_1' and D_1 it again follows that $D_1' < D_1$. However if no pronounced downstream variations were present in the streamline wave lengths and amplitudes of the initial isentropic chart, α_1 may become negligibly small over A'B because of the larger Δt in the denominator of $\partial\psi/\partial t$. In this case, the effective quarter wave length would be very nearly equal to $D_1' \doteq D_1$. This essentially implies that all other things being equal, the more distant downstream streamline features have a smaller influence on the C.A.V. trajectory than those near the initiation point.

The C.A.V. trajectory may be extended beyond B' by a continuation of the procedures described above. Moreover third approximations to the unsteady C.A.V. trajectory can be made but this may be of dubious practical value because of time limitations. In the application of these methods it would be desirable to establish a statistical relationship, if possible, without too much variance, of the form

$$\overline{\frac{\partial\psi}{\partial t}} = K\left(\frac{\partial\psi}{\partial t}\right)_{max}$$

where $(\partial\psi/\partial t)_{max}$ would be measured at the point of greatest cross-streamline angle.

The foregoing plane procedure may also be applied to spherical-type trajectories. Thus if fig. 6 refers to trajectories in spherical coordinates, it may be shown that the inflexional characteristics of OO'Q'A' are

$$\varphi_0' = \varphi_0 + \frac{\alpha h^2}{2a},$$
$$\cos\psi_0' = \frac{\cos\varphi_0}{\cos\varphi_0'}\left(\cos\psi_0 - \frac{\alpha^2 h^2}{4}\right). \tag{53}$$

Then for the second leg A'B', it may be shown that the inflexional characteristics are

$$\varphi_{1,0}' = \varphi_1 + \frac{(K_1+\alpha_1)h_1^2}{2a},$$
$$\cos\psi_{1,0}' = \frac{\cos\varphi_1}{\cos\varphi_{1,0}'}\left[\cos\psi_1 - \frac{h_1^2(K_1+\alpha_1)^2}{4}\right]. \tag{54}$$

In (53), (54) the quantities α, α_1 are measured precisely as in the plane case.

7. The correction for lateral shear

In order to correct a particular C.A.V. trajectory for lateral shear one may proceed as follows: construct the Rossby C.A.V. trajectory from the initial point O, fig. 1, (not necessarily an inflexion) and for the desired time interval. Then construct two neighboring Rossby C.A.V. trajectories initiating one from a point 5° latitude cross-stream to the left of O and the other 5° latitude cross-stream to the right. A simplified version of the three Rossby C.A.V. trajectories is presented in fig. 7 where the central C.A.V. trajectory has been depicted schematically as a straight line and the other two trajectories are drawn in relation to

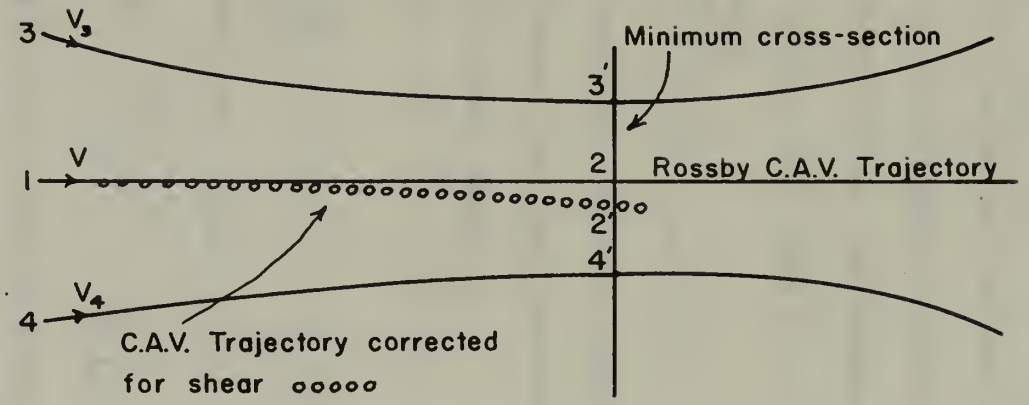

Fig. 7 Schematic method of determining lateral shear along C.A.V. trajectory.

their observed horizontal spacing from the first. From the cross-section 3-4 to 3'-4', the flow is shown as converging and thereafter diverging. For purposes of illustration, the flow is shown as possessing cyclonic shear. Then the change in the shear $\Delta(\partial V/\partial N)$, between cross-sections 3-4 and 3'-4' having normal spacing N_1 and N_2, respectively, is

$$\Delta\left(\frac{\partial V}{\partial N}\right) = \left(\frac{\partial V}{\partial N}\right)_2 - \left(\frac{\partial V}{\partial N}\right)_1 = \left(V_3 - V_4\right)\left(\frac{1}{N_2} - \frac{1}{N_1}\right). \tag{55}$$

For the Rossby C.A.V. trajectory beginning at 1 and terminating at 2, the variation of shear is zero at point 1 and has the value (55) at 2. A corrected C.A.V. trajectory between cross-sections 3-4 and 3'-4' is more nearly approximated by using a mean value of $\Delta(\partial V/\partial N)$ between 1 and 2. Let this mean value be denoted

$$\overline{\Delta(\partial V/\partial N)} = S_1 V$$

where in fig. 7, S_1 is negative. Then for points between 1 and cross-section 3'-4', an approximate form of the steady-state vorticity equation (5) (including a correction for lateral shear) is

$$\frac{V}{R} = S_1 V - (f - f_1) + K_1 V, \tag{56}$$

or

$$\frac{1}{R} = g\frac{dq/dy}{(1+q^2)^{3/2}} = K_1 + S_1 - \frac{\beta_1}{V}(y - y_1). \tag{57}$$

By analogy with (50), the first integral of (57) is

$$\cos\psi = \cos\psi_1 - \frac{(K_1+S_1)^2 h_1^2}{4} + \frac{1}{h_1^2}\left[y - y_1 - \frac{(K_1+S_1)h_1^2}{2}\right]^2, \tag{58}$$

which is a modified Rossby C.A.V. trajectory with inflexional characteristics

$$\begin{aligned} &\text{inflexional latitude:} \quad \varphi_{1,0}' = \varphi_1 + (K_1+S_1)h_1^2/2a, \\ &\text{Inflexional direction:} \quad \cos\psi_{1,0}' = \cos\psi_1 - \frac{(K_1+S_1)^2 h_1^2}{4}. \end{aligned} \tag{59}$$

If point 1 is an inflexion ($K_1 = 0$), two general types of corrected C.A.V. trajectories are possible beyond the inflexion. These types correspond

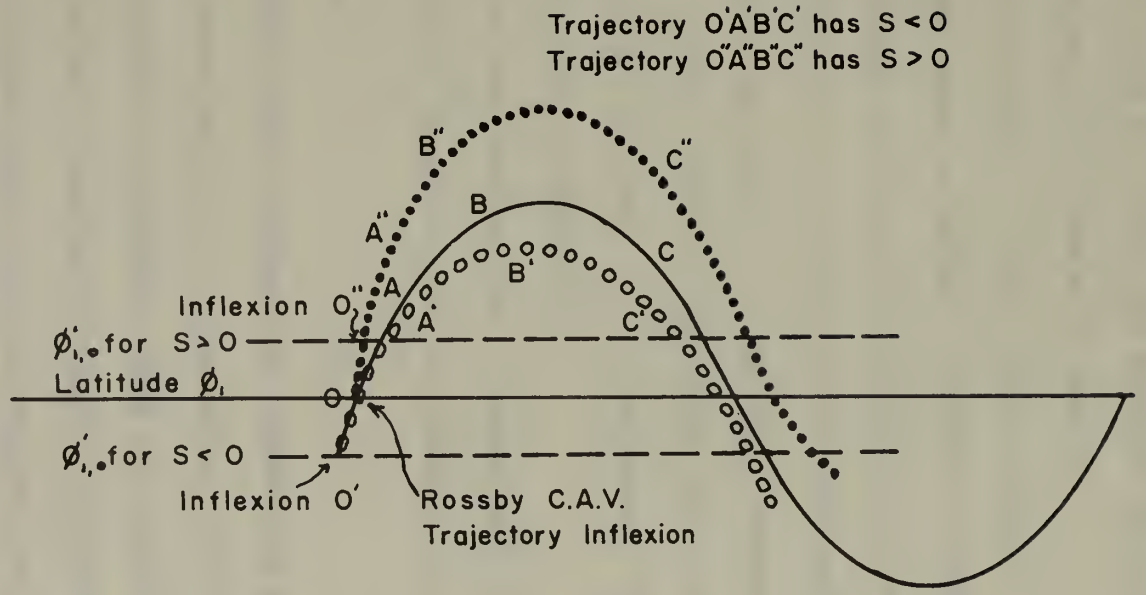

Fig. 8 Types of C.A.V. trajectories corrected for lateral shear.

to

(i) $S > 0$, increasing anticyclonic or decreasing cyclonic shear,

(ii) $S < 0$, decreasing anticyclonic or increasing cyclonic shear.

These two cases (with $S_1 = -S_2$) are depicted in fig. 8, both cases having the same inflexional directions at O' and O".

Note that the case $S < 0$, e.g. that of fig. 7, in which an increase in cyclonic shear occurs along the trajectory is attended by generally greater anticyclonic curvature (see trajectory OA'B'C' delineated by the small open circles in fig. 8) than that of the Rossby C.A.V. trajectory OABC. Conversely, the case $S > 0$, in fig. 8 corresponds to the trajectoryOA"B"C" (dotted curve in fig. 8) and has less anticyclonic curvature than that of the Rossby C.A.V. trajectory. These results are also readily apparent from equation (56).

East of the cross-section 3'-4', beyond which the sign of S reverses, the corrected C.A.V. trajectory may be extended by means of (59).

8. Conclusions

The foregoing study represents an engineering approach to the construction of generalized C.A.V. trajectories. No attempt has been made to include variations in windspeed along the trajectory. The suggested method of making the corrections for local turning and for variations in lateral shear is quasi-geostrophic in character and bears a certain resemblance to the point of view of Charney et al. in connection with the barotropic model [2]. Of course, the aim of the present article is mainly directed toward using such C.A.V. trajectories in making prognostic charts by conventional long-wave techniques rather than by electronic computers. For rapid application by Weather Centrals and other short-

range forecast offices it is planned to consolidate the Rossby graphs [9, p. 275] into a single nomogramic chart and also to incorporate the inflexional characteristics of this article, equations (36), (53) and (54), into individual nomograms. Once one has computed these characteristics, the Project ARCWA tables [12] are immediately applicable.

Finally, the full generalization of unsteady spherical C.A.V. trajectory which also has non-constant lateral shear can be obtained from (53), (54) by replacing α by $\alpha+S$ and α_1 by α_1+S_1, etc. Here

α is positive for backing winds,

S is negative for increasing cyclonic shear.

If $\alpha = -S$, the trajectory would be identical to a Rossby spherical C.A.V. trajectory having the same initial conditions. If α and S have the same sign, the C.A.V. trajectory will have an effective amplitude which may depart considerably from that of the Rossby C.A.V. trajectory.

In view of Sutcliffe's equation (3) these methods should also be applicable with sufficient accuracy to trajectories drawn on isobaric charts near the level of non-divergence.

REFERENCES

1. Carlstead, E. M., 1953: A study of constant absolute vorticity trajectories on an isentropic surface. J. Meteor., 10, 356-361.

2. Charney, J. G., Fjortoft, R., and Neumann, J. v., 1950: Numerical integration of the barotropic vorticity equation. Tellus 2, 237-254.

3. Fultz, D., 1945: Upper air trajectories and weather forecasting. Dept. Meteor., Univ. Chicago, Misc. Rep., No. 19, 121 pp.

4. Haltiner, G. J., 1951: The isentropic absolute vorticity equation (unpublished manuscript), 2 pp.

5. Grant, A. M. 1953: The effect of the steady-state assumption on constant vorticity trajectories. J. Meteor., 10, 397-398.

6. Platzman, G. W., 1947: Some remarks on the measurement of curvature and vorticity. J. Meteor., 4, 58-62.

7. Riehl, H. et al, 1952: Forecasting in middle latitudes. Met. Monographs I, No. 5. Amer. Met. Soc., Boston, Mass., pp. 1-80.

8. Rossby, C. G., 1940: Planetary flow patterns in the atmosphere. Quart. J. r. meteor. Soc., 66 (supplement), 68-87.

9. _____, 1942: Forecasting of flow patterns in the free atmosphere by a trajectory method. Appendix to Basic principles of weather forecasting by V. P. Starr, New York, Harper & Bros., 268-284.

10. Starr, V. P., 1945: A quasi-Lagrangian system of hydrodynamical equations. J. Meteor., 2, 227-237.

11. Sutcliffe, R. C., 1947: A contribution to the problem of development. Quart. J. r. meteor. Soc., 73, 370-383.

12. U.S. Navy Bureau of Aeronautics, Project AROWA, 1952: Topical outline of refresher course for reserve aerologists in recent developments in upper air analysis and forecasting. Norfolk, Section 7.

TA7 27443
.U6 Martin
no.7 Generalization of constant absolute vorticity trajectories.